MINISTRY OF EDUCATION AND TRAINING

VIETNAM ACADEMY OF SCIENCE AND TECHNOLOGY

GRADUATE UNIVERSITY OF SCIENCE AND TECHNOLOGY

Nguyen Thanh Hoang

MONTE CARLO SIMULATION OF MAGNETIC MICROSPHERES Fe_3O_4/POLY(GLYCIDYL METHACRYLATE)

SUMMARY OF DISSERTATION ON OPTICAL, OPTOELECTRONICS AND PHOTONICS MATERIALS
Code: 9440127

Ho Chi Minh city – 2024

The dissertation is completed at: Graduate University of Science and Technology, Vietnam Academy Science and Technology

Supervisors:

1. Supervisor 1: Assoc. Prof. Dr Nguyen Manh Tuan

2. Supervisor 2: Assoc. Prof. Dr Tran Hoang Hai

Referee 1: .....

Referee 2: .....

Referee 3: .....

The dissertation is examined by Examination Board of Graduate University of Science and Technology, Vietnam Academy of Science and Technology at … hour …', date … month … year 202…

INTRODUCTION

1. The urgency of the thesis

Over the past decade, nanocomposite materials have been researched and widely applied based on novel properties such as flexibility, combining many advantages of the component materials and background material to increase the bioavailability and efficiency of applications. With these advantages, the composite materials contained magnetic nanoparticles embedded in a biodegradable polymer shell applied to many applications, namely biological labeling, microfluidics, targeted drug delivery systems, and local hyperthermia. They showed great potential in fields like biopharmaceuticals, biomedicine, and others.

In applications using external magnetic fields, particularly in the biomedical field, the survey, analysis, and evaluation of magnetic properties, intrinsic microscopic parameters such as magnetic anisotropy, torque, and blocking temperature of these materials are pivotal and the main factors that govern the effectiveness of the materials. Therefore, accurately determining the size distribution function, the influence of the matrix material, and the role of the dipolar interaction of magnetic nanoparticles within the composite material plays a key role.

On the one hand, although modern experimental analysis methods have the advantage of being intuitive and can qualify and quantify macroscopic quantities, they are costly in terms of time, human resources, material resources, repeatability not high, and many expensive equipment have yet to be equipped. Besides, experiments and measurements under particular conditions (very high or absolute temperature 0 K, ultrafast laser pulse) are sometimes complex. In addition, the materials have microscopic levels in the dimensions, which has led to the quantifying of measured parameters becoming a challenge for experimental measurement methods.

On the other hand, magnetic theories have had a long history of formation and development alongside intuitive experiments, which generalize and create a solid foundation for research and applications of materials in practice. From there, it built powerful computational tools that not only contribute to solving the limitations of experiments but also create mathematical models - framework of computer simulations, allowing not only training to study the intrinsic micromagnetic properties of materials further but also to be able to conduct experiments at a low cost, liberate the researcher's labour, have high repeatability, shorten research time, and be able to predict the macroscopic properties of materials. In the past decade, high-performance computer systems and supercomputers have been born with superior configurations combined with powerful parallel computing algorithms, allowing calculate and simulate macroscopic systems (actual samples) from parameters at the microscopic (atomic) level with numbers up to billions of atoms. In addition, the quantum computer system was born recently, further promoting the excellent potential for computational and simulation research for science in general and materials science in particular. In addition, the achievements of the fourth industrial revolution with modern techniques such as big data and machine learning have opened up new research directions full of potential benefits—a priori in the design and research of materials. However, many properties and phenomena of materials occur on two or more scales in both space and time. This causes a lack of information, incomplete evaluation in experimental studies or the use of approximations in pure calculations/computer simulations, which, if attempted to be complete, will waste time and money. Lack of mutual reference between experimental results, theory and simulation calculations leads to the obtained results becoming "disjointed". To solve that problem, combining experimental research, theory and computer simulation to investigate the properties of materials is gradually becoming a new trend worldwide.

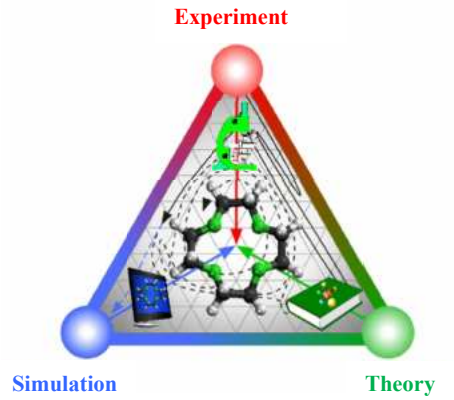

The correlation between experiment, theory and computers simulation in materials science.

2. Research objectives of the thesis

With the desire to build a model to study magnetic properties for common composite material structures that are applied to current biomedical applications such as liposomes, microspheres, microcapsules, micelles, dendrimers, including both carbon-based materials (CNT, Graphene), the author tries to conduct multi-dimensional research combining experiments, magnetic theory and computer simulations to forming a model that allows investigating, quantify and evaluate in the most detail possible the intrinsic micromagnetic properties of the composite materials. Based on our previous research, a simple composite material used in many fields to facilitate surveying and concretization without losing the model's generality, such as microspheres containing Fe_3O_4 magnetic nanoparticles, was selected as a specific investigation object. From there, the author carried out the thesis *"Monte Carlo simulation of Fe_3O_4/Poly(glycidyl methacrylate) magnetic microsphere system"*. Due to regulations on name editing, the thesis name does not include the entire work performed by the doctor of philosophy student on this thesis. The thesis content below will fully demonstrate the work sequence in this research.

3. Main research contents of the thesis

Firstly, in this work, the author presents experimental methods to fabricate and measure the initial macroscopic characteristics of the Fe_3O_4/Poly(glycidyl methacrylate) microsphere material in this work.

In the next part, the author employs precise numerical calculations based on magnetic theories to investigate the intrinsic parameters of the synthesized materials, such as the particle size distribution function and effective magnetic anisotropy constant. These important parameters, combined with experimental results, will become input parameters for computer simulations to most accurately represent the Fe_3O_4/Poly(glycidyl methacrylate) microsphere material, thereby assuring the accuracy of the simulation results.

Finally, the author applies practical computer simulation methods (Monte Carlo and atomic spin model simulations) to investigate, evaluate, and quantify the intrinsic micromagnetism parameters and the complex magnetic dynamic behaviour of the microsphere material. From the results obtained, the author strives to provide some essential predictions for the experiment, emphasizing the relevance of the research.

CHAPTER 1. OVERVIEW

1.1. Magnetic Microspheres Fe_3O_4/Poly(Glycidyl Methacrylate)

Poly (Glycidyl Methacrylate) (PGMA) is a fascinating polymer widely used in industrial and biomedical fields. Its unique characteristics, such as being inexpensive, biocompatible and non-toxic, and its

ability to self-assemble, biodegrade and respond to pH changes, make it a versatile material. The morphology of PGMA derivatives is particularly intriguing, as it can create complex structures through self-assembly, including micelles (spherical, cylindrical...), island micelles (RM), capsules and nanoparticles [5]. The effects of various internal and external factors, such as the length and ratio of the hydrophobic part, pH, solvent composition, and temperature, can further alter their morphology [6]. This adaptability, hydrophilicity, and ease with which its epoxy groups can be modified to carry reactive functional groups make PGMA a promising material for various applications, including nanomedicine, biotechnology, and molecular biology [7].

The use of Fe_3O_4 magnetic nanoparticles in combination with PGMA further enhances the potential of these materials. This dispersion process not only prevents the accumulation of magnetic nanoparticles, which can affect the magnetic properties of materials [8], but also opens up new possibilities in nanomedicine, biotechnology, and molecular biology [9]. The versatility and potential of these materials are genuinely inspiring, offering exciting opportunities for future research and applications.

1.1.1. Structural components

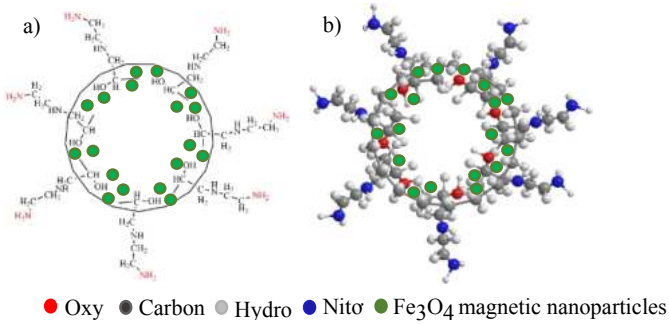

Figure 1.2. Model illustration of 2D (a) and 3D (b)

1.1.2. Poly(Glycidyl Methacrylate) background material

-Commonly nomenclature: Poly(Glycidyl Methacrylate); 2 - Propenoic acid, 2 - methyl-, oxiranylmethyl ester.

- Molecular formula: $(C_7H_{10}O_3)_n$

-M_n = 10.000-20.000 (đvC)

-Characteristics: biodegradable and pH-sensitive, poly (glycidyl methacrylate), curing or swelling when there is a change in pH of the surrounding environment, can create block copolymers), is capable of responding to more than one type of stimulus from the external environment (dual responsive), has a spherical shape, is relatively uniform in size, and is less likely to agglomerate, so it is used as a dispersing agent. In addition, the surface is easily modified to create additional amino functional groups NH_2-, the surface area is large, and the hydrophobic tail turns inside the core, forming a space between the microspheres. Recently, it has been used in MEM (Micro Electro Mechanical) technology to package chips used in the human body or in systems that interact with biological particles.

1.1.3. Component materials: Fe_3O_4 magnetic nanoparticles

Magnetic iron oxide Fe_3O_4 is a mixed oxide $FeO.Fe_2O_3$ - belongs to the group of magnetic ceramics called Ferrite. A regular unit cell has 8 tetrahedral sites and 16 octahedral sites.

A specific magnetic material system will exist in different magnetic energy forms - the sum of all magnetic energy contributing to the total energy formation system. Minimizing the total energy will determine the domain structure of the magnetic nanoparticle. This parameter is critical during computer simulations of magnetic materials.

1.1.4. Potential applications of Fe_3O_4/Poly(Glycidyl Methacrylate) magnetic microspheres materials.

Fe_3O_4/Poly(Glycidyl Methacrylate) microsphere materials are currently being widely used in novel biomedical applications that use external magnetic fields such as: targeted drug delivery, local hyperthermia, microfluidics and water treatment (adsorption of heavy metal ions). This shows the great potential of the microsphere materials.

1.2. Computer simulation in materials science

Computer simulation is the use of computers to simulate (imitate) events/phenomena in nature (system) based on a previously built model (analytical model).

The computer simulation process requires a deep understanding of technical details such as the model's initial state, boundary conditions, and interaction potential. These factors are the very foundation of the simulation, dictating its behaviour and outcomes. The primary steps of the process involve building a model → programming → conducting a test run → referring to the results. The previously built model and the desired results heavily influence the program's construction. Numerous software options are available, both free and commercial, many of which come packaged with libraries such as Materials Studio, GROMACS, LAMMPS, Quantum ESPRESSO, and VASP. Alternatively, you can build your simulation using popular programming languages like C++, Matlab, and Python.

1.3. Research state of affairs

1.3.1. Domestic

To the author's knowledge, no research has been recorded on the PGMA magnetic microsphere material system from experiment and theory to computer simulation.

1.3.2. In the world

Research by scholars around the world has shown the potential application of PGMA magnetic microsphere material in biomedicine. Investigation of their characteristics using experimental analysis methods and "in-vitro" experiments has also been carried out. However, the magnetic properties of PGMA magnetic microsphere material still need to be investigated and performed thoroughly.

In this thesis, the author embarks on a novel exploration of the magnetic properties of the Fe_3O_4/PGMA microsphere material. The unique aspect of this research is that the magnetic properties of the microsphere material are entirely dependent on the magnetic properties of Fe_3O_4 magnetic nanoparticles distributed within the non-magnetic PGMA polymer matrix. The author will synthesize Fe_3O_4/PGMA magnetic microspheres and employ various experimental and analytical methods to investigate their characteristics, all while minimizing costs. The author will also use numerical calculation methods to estimate the intrinsic micromagnetic parameters of the microsphere materials, such as the magnetic anisotropy constant and the particle size distribution of Fe_3O_4 magnetic nanoparticles within the microspheres. The author posits that dipolar interactions between Fe_3O_4 magnetic nanoparticles will significantly impact their distribution within the PGMA polymer matrix.

Furthermore, the Monte Carlo simulation underscores the role of dipolar interactions in influencing the magnetic properties of microsphere materials, which unequivocally demonstrates the existence of dipolar interaction between Fe_3O_4 magnetic nanoparticles loaded in microspheres. This simulation serves as a crucial validation of the research findings. Moving forward, the investigation will delve into other parameters such as torque, magnetic moment distribution of magnetic nanoparticles, the influence of magnetic nanoparticle size on the magnetic properties of the material system, the role and influence of magnetic nanoparticles, and the effect of dipolar interaction on the magnetic properties of the material. The atomistic spin model simulations will be performed based on input data, which are results obtained from experiments and numerical calculations.

Using computer simulation methods is essential to overcome significant barriers posed by dipolar effects, such as constraining the direction of measurement and changing the size/distance between magnetic nanoparticles in microspheres. The generalization of the research methods of the thesis is described in Figure 1.28, and details of each implementation process will be presented by the author in detail in the following chapters.

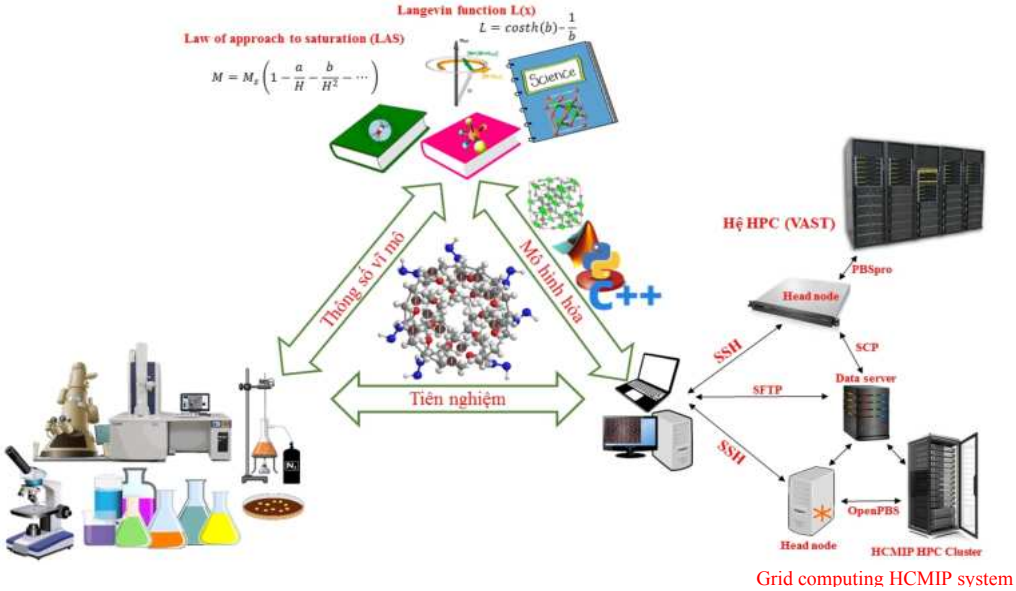

Figure 1.28. Overview of the research methods of the thesis
The multidimensional research: Experiment, theory and simulation.

CHAPTER 2. RESEARCH METHODS

2.1.Experiment

2.1.1. Synthetic process

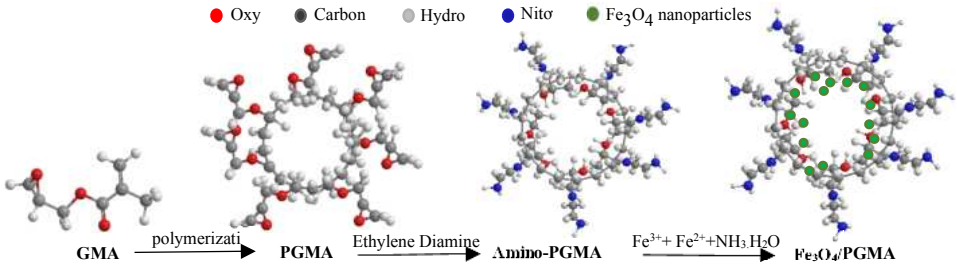

Figure 2.1. Diagram depicting the synthesis process of Fe_3O_4/PGMA magnetic microsphere materials.

2.1.2. Analytical methods

Modern and basic measurement methods used to obtain the essential characteristics of synthesized materials such as X-ray diffraction (XRD), Fourier transform infrared spectroscopy (FTIR), magnetic Vibration spectrometer (VSM), scanning electron microscope (SEM), transmission electron microscope (TEM), atomic absorption spectroscopy (AAS).

2.2. Numerical calculations

2.2.1. The Law of approach to saturation - LAS

2.2.2. Fitting to the Langevin function

2.2.3. Programs for number calculation and presenting results

2.3. Computer simulations

2.3.1. Monte Carlo (MC) simulation

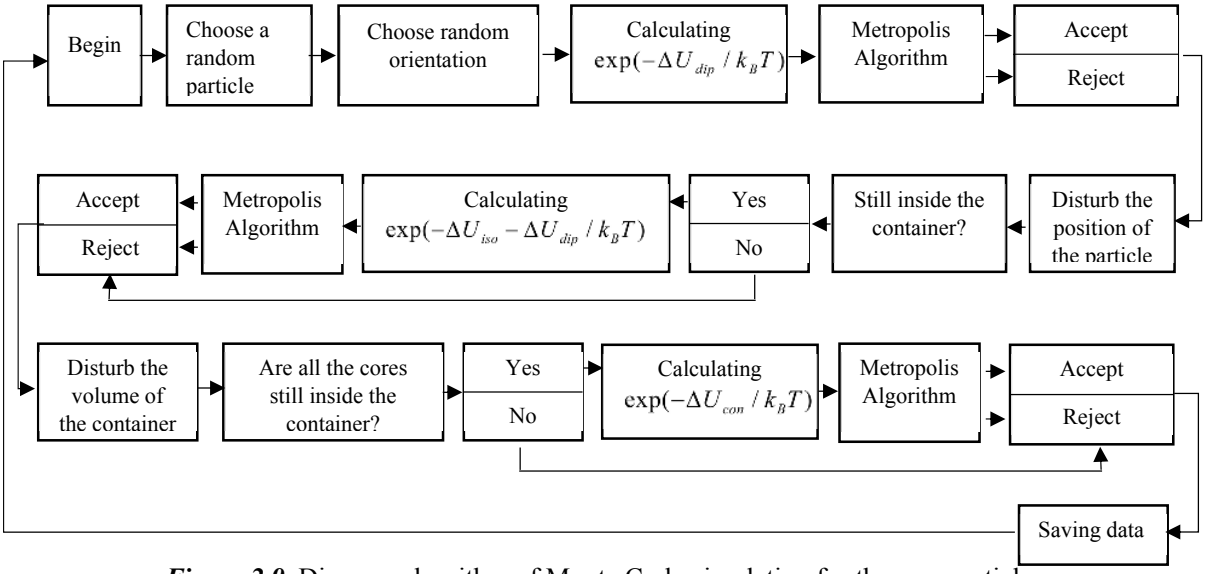

Figure 2.9. Diagram algorithm of Monte Carlo simulation for the nanoparticles Fe_3O_4 loaded inside microspheres PGMA.

The pressure constant MC simulation method [87,88] is used to simulate the forming of Fe_3O_4 nanoparticle clusters inside the PGMA magnetic microsphere material. To perform the simulation, we must first build mathematical models. In the experimental steps of material synthesis presented in the previous part of the thesis, the Fe_3O_4 nanoparticles were formed by in situ precipitation inside the PGMA polymer matrix. They are stably dispersed inside the colloidal form (PGMA polymer matrix), so we will apply the DLVO theory [89] to describe the isotropic interactions between magnetic nanoparticles, including Van der Waals affinity, electrostatic repulsion and include the Pauli exclusion principle [90].

2.3.2. Atomistic spin model simulation

Atomistic spin model simulations are a powerful tool in our arsenal. They treat atoms as having a local magnetic moment and couple electronic theory to the equations of motion of atomic spins [94]. This approach bridges the gap between micromagnetic and ab initio simulation methods, enabling us to delve into the intricate world of detailed microscopic properties. We can explore complexities such as surface anisotropy, spin dynamics triggered by ultrafast laser pulses, exchange bias in core-shell magnetic nanoparticles, multilayer magnetic thin films, and spin torque [95].

We can utilize atomistic spin model simulation packages like VAMPIRE to leverage existing platforms and avoid code development from scratch. While its functions are still under development [90], VAMPIRE stands out for its unique features. It is built on crucial magnetic theories, employing the extended Heisenberg spin model and the fundamental physical principles of magnetic materials at the atomic scale, such as the classical spin Hamiltonian as in the Ising model. Moreover, it incorporates atomic spin dynamics based on the Landau-Lifshizt-Gilbert and Langevin equations. VAMPIRE operates with input files comprising three types (unit cell, material, and input). Magnetic quantities in the software package are specified according to specific standards and, when referencing experimental results, need to be converted to the international system of units (SI system).

2.3.3. Modern facilities to perform simulations

2.3.3.1. High performance computing system

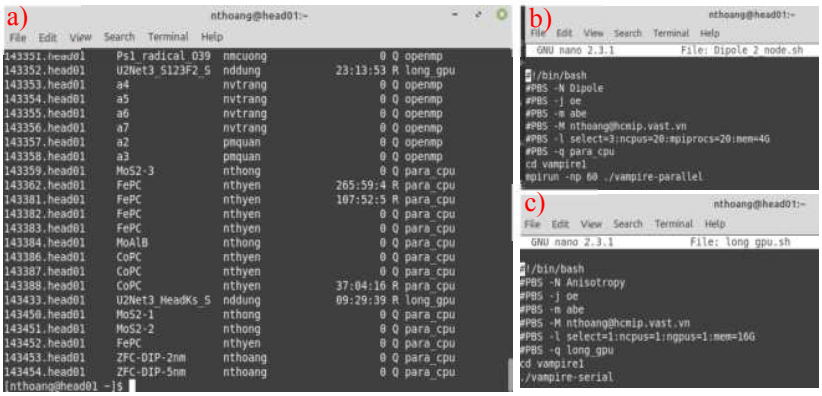

Figure 2.12. VAST HPC system

(a) Workload manager & Jobs scheduler of the VAST HPC system

(b) (b, c) Script files to run simulations on VAST HPC system.

The simulations in this thesis were performed on the high-performance computing (HPC) system of the Center for Informatics and Computing - Vietnam Academy of Science & Technology (VAST) through the Secure Shell protocol (SSH).) using Terminal on the Linux operating system (Figure 2.12) or Cmd/Windows subsystem for Linux – WSL on the Windows platform.

Monte Carlo simulations must run in single-core mode (Serial), while other simulations are run in multi-core mode (Para CPU) and compute in parallel on 2-3 nodes (Each node has 20 cores). To speed up calculation. Or run on the Tesla P100 GPU card to reduce calculation time.

2.3.3.2. Grid computing system

Recently, due to the increasing need to perform computational research, the number of users ($USER) on the HPC-VAST system has increased significantly. To ensure work needs as well as to develop a high-performance computing model in the direction of modernization, sharing resources widely and meeting techniques such as big data (Big data), machine learning (Machine learning) as well as covering modern computing architecture such as cloud computing (Cloud computing) for computer simulations to research materials science in particular and other aspects of science in general, The author has built a hybrid computing system for high-performance computing including a small cluster (Appendix IX) consisting of Worker Nodes (CPU and GPU) computing, a Master Node concurrently Web Server and a Data Server based on grid computing architecture [101,102]. The system is located at the Ho Chi Minh City Institute of Physics - VAST (details at http://hcmip.ac.vn/hpc); the next phase will test the direct submission of jobs on the Web backend 3.0 platform without The need to use complicated script files to simplify and aim for user-friendliness. After completing the simulation calculation data on the system, it will be automatically pushed to the Data Server; from there, the data will be downloaded to the personal computer (client) via SCP (secure copy) or SFTP (Secure File) protocol. Transfer Protocol). In addition, for consolidation and convenience in storage, calculation data will be transmitted to this data server via the SCP protocol after being performed on the HPC-VAST system.

The advantage of this computing system is that it can perform and manage simulated Jobs and calculations on the system on many device platforms, from smartphones and tablets to personal computers. In addition, data will be recorded and sorted into the storage system (Server Data), and supervised learning techniques (Supervised Learning) can be used to perform automatic classification - an essential step of the

machine learning process. After being classified, these data can be regressed to provide priors within the allowable capacity.

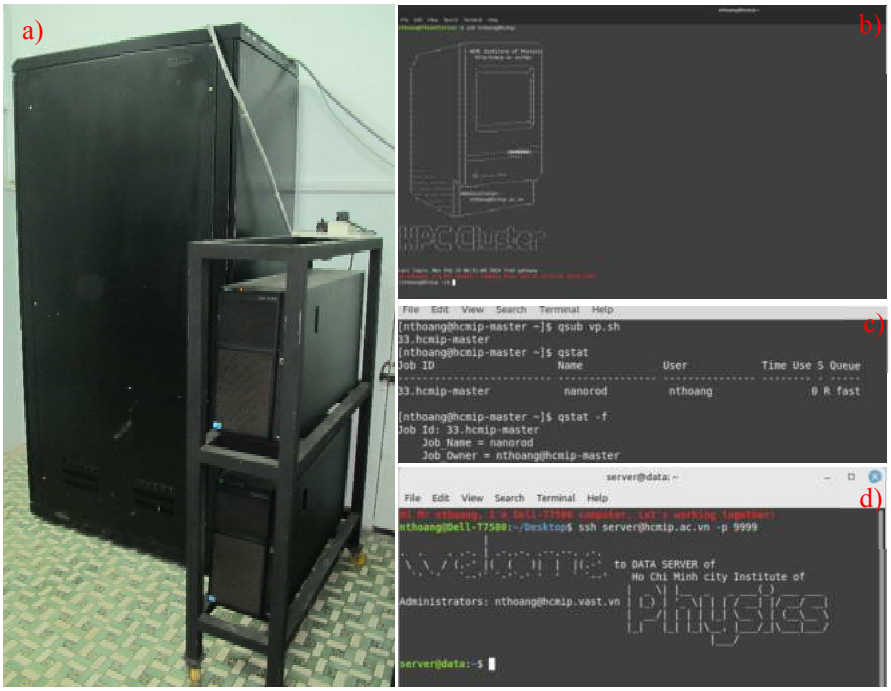

Figure 2.13. HCMIP grid computing system

(a) HCMIP grid computing system

(b, c) Workload manager & Jobs scheduler of the HPC Cluster in the grid computing system

(d) Server Data in grid computing system.

Due to increased computational demand and expansion of research on quantum computing (Quantum computing) in physical chemistry and materials science, pre-simulation calculations have been run before running online. Continuing on IBM's quantum computer, the author built an additional high-performance computing system, Comphys (Figure 2.14), to facilitate research work (Appendix X). The structure is similar to the HCMIP system above but has been upgraded with many new functions to support quantum calculations.

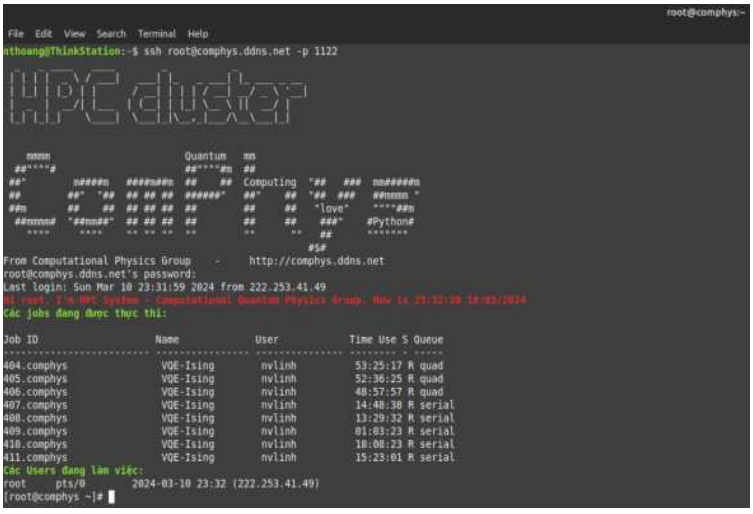

Figure 2.14. Comphys computing system.

CHAPTER 3. RESULTS AND DISCUSSION

3.1. Experimental results and numerical calculations

3.1.1. X-ray diffraction (XRD)

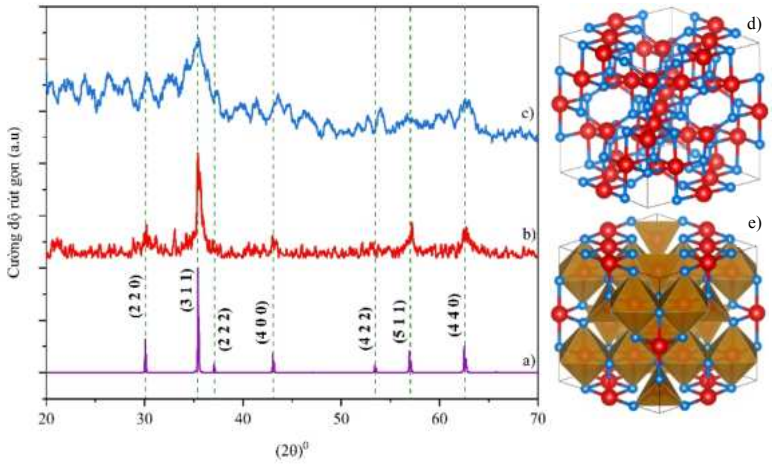

Figure 3.1. X-ray diffraction pattern of: (a) Standard spectrum of Fe_3O_4 (b) bare Fe_3O_4 nanoparticles; (c) Fe_3O_4/PGMA microspheres material (d, e) Unit cell and polyhedral unit cell of Fe_3O_4.

Figure 3.1 shows the X-ray diffraction pattern of the samples: (b) bare Fe_3O_4 nanoparticles (not coated with PGMA) and (c) synthesized Fe_3O_4/PGMA material. According to the X-ray diffraction diagram (Figure 3.1b, c), the diffraction peaks are at the surfaces lattice (2 2 0), (3 1 1), (4 0 0), (4 2 2), (5 1 1) and (4 4 0) coincide with the standard XRD spectrum data for Fe_3O_4 (JCPDS card No.75-0033 – figure 3.1a). Observing Figure 3.1c, no other phase composition was found, which proves that pure Fe_3O_4 particles were formed inside the PGMA microspheres. However, the X-ray diffraction intensity is reduced here, and the diffraction peak is broadened compared to Figure 3.1b. The initial assumption is that the cause may be the Fe_3O_4 particles forming inside the Fe_3O_4/PGMA microspheres with small crystal size, this has been discussed in [103]. Additionally, the presence of a PGMA matrix on the surface of Fe3O4 particles increases the perturbation in the structure [104]. Another reason is that when distributed inside/on the surface of Fe_3O_4/PGMA microspheres, Fe_3O_4 nanoparticles were fixed by the PGMA polymer matrix, reducing the ability to agglomerate into large clusters. At the same time, they are widely dispersed, thereby making the particle density lower than that of bare Fe_3O_4 particles. As a result, the diffraction peak height is reduced, and the width of the diffraction peak is also widened, which has also been discussed by Majid Sakhi Jabir and colleagues [105]. The Scherrer equation obtained the average crystallite size (d_{XRD}) of the bare Fe_3O_4 particles as $d_{Fe_3O_4}$= 15.8 (nm).

Figure 3.2 refers to the X-ray diffraction diagram of the fabricated Fe_3O_4/PGMA material and the background PGMA polymer, We see that at the diffraction angle of $2\theta = 17^o$, a unique diffraction peak characteristic of the PGMA polymer material appears [106]; this proves that the synthesized Fe_3O_4/PGMA material has two precise components, including PGMA polymer background material and Fe_3O_4 nanoparticles component material.

Determining the crystallite size of Fe3O4 particles dispersed inside Fe_3O_4/PGMA microspheres by the Scherrer approach (the small size of these particles as discussed above will cause significant error due to the effect of broadening the diffraction peak width), a highly accurate method such as Small Angle X-Ray Scattering (SAXS) can be used. On the one hand, the thesis has been unable to carry out these measurements due to unfavourable conditions. On the other hand, the crucial experimental parameter needed to feed the

computer simulations performed later in the thesis is the magnetic core size and not the crystal size, so another method is based on In theory, magnetism will be used to obtain parameters about the magnetic core size, details are presented below.

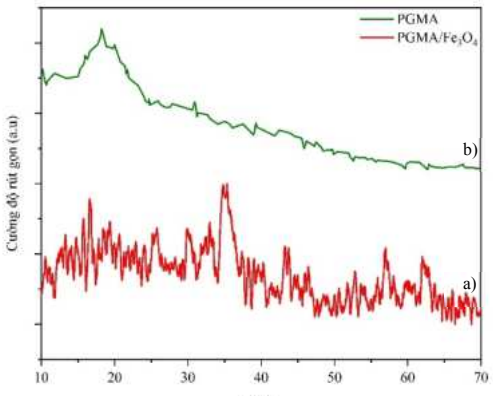

Figure 3.2. X-ray diffraction pattern of:
(a) Fe_3O_4/PGMA microspheres; (b) Polymer PGMA [106].

3.1.2. Fourier-transform infrared spectroscopy (FTIR)

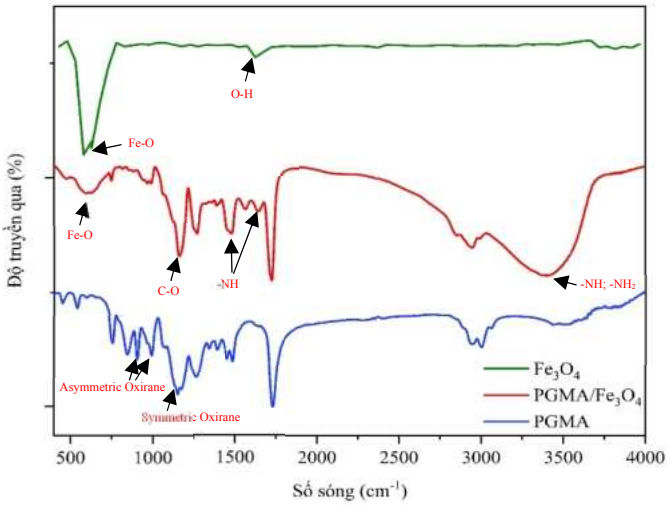

Figure 3.3. FTIR spectra of the samples in transmission mode
PGMA; (b) Fe_3O_4/PGMA; (c) Fe_3O_4 [107].

The FTIR spectrum of pure PGMA (Figure 3.3a) shows that characteristic absorption regions appear at the wavenumber positions 1149 cm^{-1} and 846 cm^{-1}, 993 cm^{-1} respectively, related to the symmetric oxirane rings (-CH_2-O-CH_2-) and asymmetric oxirane rings (-CH_2-O-CH-) (epoxides) (Figure 3.4a). Besides, stretch vibration of the carbonyl functional group (C=O) in PGMA appears at wave number 1730 cm^{-1}.

However, the FTIR spectrum of Fe_3O_4/PGMA in Figure 3.3b shows that the dips at 846 cm^{-1} and 993 cm^{-1} almost disappear, characteristically corresponding to the asymmetric oxirane ring (-CH_2-O-CH-). Besides, the appearance of new absorption bands at 3399 cm^{-1}, 1566 cm^{-1} and 1644 cm^{-1} corresponds to the stretching and bending vibrations of N-H and stretching of N-H_2, demonstrating the presence of functional groups -NH and -NH_2, as a result of the modification of PGMA by Ethylenediamine, causing the epoxides (oxirane rings) to open the ring (Figure 3.4b). On the other hand, the presence of a new absorption band observed at 592 cm^{-1} in Figure 3.3b corresponds to the vibration of the Fe-O bond (observe FTIR spectrum of pure Fe_3O_4 in Figure

3.3c [107], proving the existence of Fe_3O_4 magnetic nanoparticles in PGMA microspheres. On the other hand, the slope observed at 1130 cm^{-1} corresponding to the vibration of the functional group (C-O) is shifted to the high-frequency region. Furthermore, this suggests that the PGMA polymer interacts with the metal ions of Fe_3O_4 and immobilizes them (adsorption interaction by intermolecular forces → formation of coordination bonds); similar results were reported by Author Jana Koubkova and colleagues [108].

3.1.3. Scanning electron microscopy (SEM) image

The particle size distribution function of Fe_3O_4/PGMA magnetic microspheres (Figure 3.6d) was determined by measuring the diameter of 100 particles from SEM images, then represented by a bar graph. Then, it fitted the histogram with a log-normal distribution function.

SEM image of the Fe_3O_4/PGMA magnetic microspheres in figure 3.6a, b show that the synthesized Fe_3O_4/PGMA material is spherical in morphology, monodisperse and quite uniform in size. Besides, the surface of Fe_3O_4/PGMA microspheres is rough due to the modification of the PGMA microsphere surface with Ethylenediamine and Fe_3O_4 magnetic nanoparticles on the surface. The average size of the synthesized Fe_3O_4/PGMA microspheres is $\langle D \rangle_{SEM}$ = 1.36 µm , and the corresponding standard deviation is σ_{SEM} = 0.09 µm. Kết quả này nhỏ hơn so với báo cáo của các nhóm tác giả khác [62,63,65,67,68]. This result is smaller than that reported by other groups of authors [62,63,65,67,68]. A simple program written by the author in Matlab with input is parameters obtained from the SEM image above to represent Fe_3O_4/PGMA microspheres in 3-dimensional space, limited to a 10×10×10 µm box (figure 3.6c).

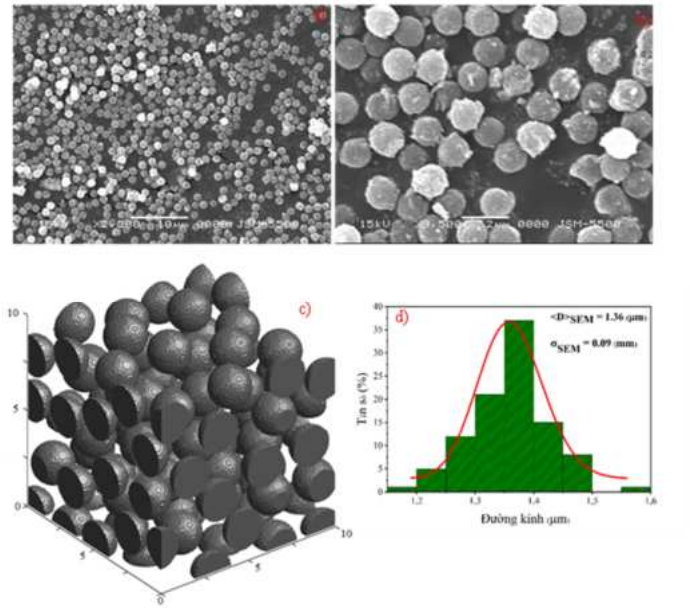

Figure 3.6. SEM image of Fe_3O_4/PGMA microspheres at 2 scales: (a) 10 µm and (b) 2 µm.
(c) Model representing Fe_3O_4/PGMA microspheres in 3-dimensional space (Matlab)
(d) Particle size distribution histogram and logarithmic-normal distribution function (solid line).

3.1.4. Transmission electron microscopy (TEM) image

As the problem raised in the previous part of the thesis, the resolution of TEM images still does not allow us to accurately determine the particle size and size distribution function of Fe_3O_4 particles inside the synthesized Fe_3O_4/PGMA material. Suppose that more modern microscopic techniques (such as HRTEM with higher resolution) can give us better observations, and from there, we can temporarily determine the size distribution. However, the size and distribution function obtained only consider one microsphere. They, therefore, cannot represent all microspheres within the synthesized sample. In other words, it is only local and

not meaningful regarding statistics. Therefore, how to accurately determine particle size and the corresponding size distribution function will be presented below.

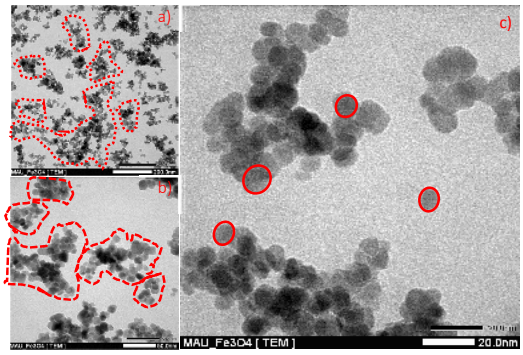

Figure 3.7. TEM images of the bare Fe_3O_4 nanoparticles at various scales:
a) 200 nm; b) 50 nm; c) 20 nm.

For the vital purpose of visually observing the shape and agglomeration of the Fe_3O_4 magnetic nanoparticles in the PGMA polymer matrix to use these parameters for other research steps of the thesis, we proceed with the fabrication according to the experimental cycle like the experimental part of the thesis without using Ethylene Diamine, coating on silicon substrate then drying and taking TEM images of the material sample (Figure 3.7). This method cannot completely represent the formation and aggregation process of the Fe_3O_4 nanoparticles inside the Fe_3O_4/PGMA microsphere material we are considering since we have broken the mesoscopic structure of the material. However, the purpose of this method is only to accurately and intuitively observe the geometry of Fe_3O_4 magnetic nanoparticles to provide accurate models in numerical theoretical calculations as well as computer simulations performed - material in the later part of the thesis. Besides, we can also observe the agglomeration of the Fe_3O_4 nanoparticles under the effect of interparticle interactions, different shapes/sizes of particle clusters, and at the same time, derive suggestive information about the number of Fe_3O_4 particles in a cluster.

Observing TEM images at scales 200 nm and 50 nm (Figure 3.7a, b), it can be seen that the nanoparticles from Fe3O4 are not uniformly distributed but aggregate into clusters of different sizes and shapes (dashed line). A dipolar interaction exists between Fe3O4 magnetic nanoparticles, which causes the particles to agglomerate into particle clusters or chains [111] and directly affects the performance of local hyperthermia applications [112]. To investigate the dipolar interaction between Fe3O4 magnetic nanoparticles, the ferromagnetic resonance (FMR) technique can be used [113,114]. However, this technique is complex; the following part of the thesis will present a more straightforward method.

Besides, TEM images at a 20 nm scale show that the Fe_3O_4 nanoparticles have an almost spherical elliptical shape (Figure 3.7c). To simplify the calculation and simulation process, we assume that the Fe_3O_4 particle is spherical with a diameter and a standard logarithmic distribution function obtained from the fitting to Langevin function approach presented in the previous part of the thesis.

3.1.5. Magnetization curves

Fe_3O_4/PGMA microspheres have superparamagnetic behaviour (Figure 3.8a). The saturation magnetization (M_s), remnant magnetization (M_r), and coercive field (H_c) obtained from the magnetization curve are listed in Table 2.5. Magnetic nanoparticles are shaped inside PGMA, under the effect of the PGMA polymer matrix on the surface atoms, forming disordered magnetic layers (will be presented in detail below)→ dramatically reducing the strength of saturation magnetization compared to the bare Fe_3O_4 nanoparticles

(Figure 3.8b). Similar results for FeCo nanoparticles were also discussed by Davide Peddis and colleagues [118].

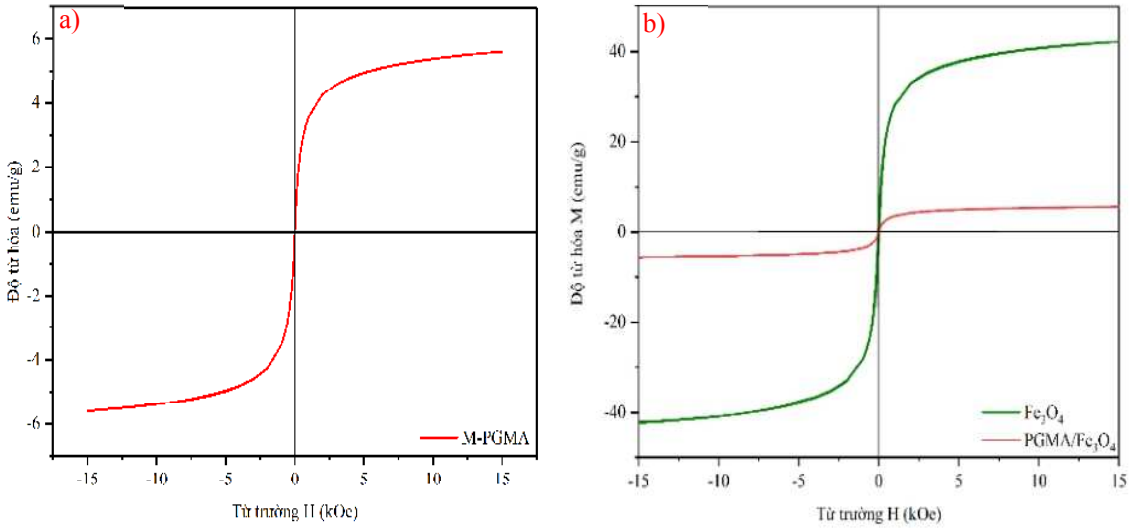

Figure 3.8. Magneitzation curves M(H) at room temperature (300 K) of:
(a) the Fe_3O_4/PGMA microspheres
(b) the Fe_3O_4/PGMA microspheres and the bare Fe_3O_4 nanoparticles.

Table 2.5. Magnetism parameters of the Fe_3O_4/PGMA microspheres.

M_s(emu/g)	H_c (Oe)	M_r (emu/g)	K_{eff} (LAS) ($\times 10^3$ J.m^{-3})	K_{eff} (T_B) ($\times 10^4$ J.m^{-3})
5.61	1.42	0.015	2.9 ± 0.6	1.9 ± 0.15

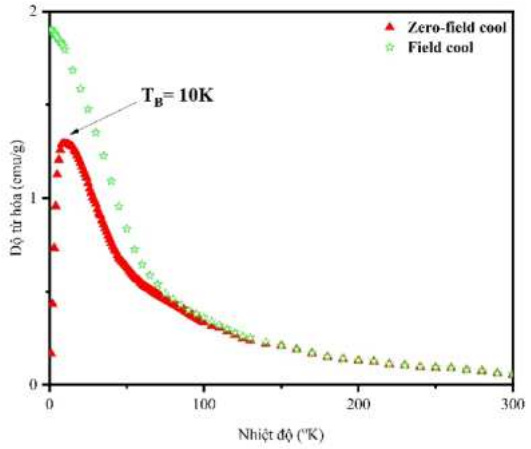

Figure 3.9. ZFC/FC magnetization curves of the Fe_3O_4/PGMA microspheres.

ZFC/FC magnetization curves of the Fe_3O_4/PGMA microspheres (figure 3.9) show that blocking temperature (T_B) (peak of the ZFC curve) →T_B= 10 K → effective magnetic anisotropy constant K_{eff} = 19 kJ/m^3, This value is approximately the same as the results reported by other scholars (10-20 kJ/m^3) for bare Fe_3O_4 particles (size ~ 5-8 nm) and larger than compared to bulk Fe_3O_4 materials (1.1 $\times 10^4$ J/m^3) [123-131]. The main reason is due to the dependence of Keff on the particle size of the Fe_3O_4 nanoparticles (K_{eff} increases as the particle size decreases); this has also been discussed by author Abdel-Fatah Lehlooh and colleagues [132], authors C. Nayek et al. [133]. Specifically, it is explained by the increase in surface anisotropy (K_s) as

the grain size decreases (as the grain size decreases, the ratio between surface and volume increases, leading to a rise in surface anisotropy).

3.1.6. Numerical calculations

3.1.6.1. Law of approach to saturation (LAS)

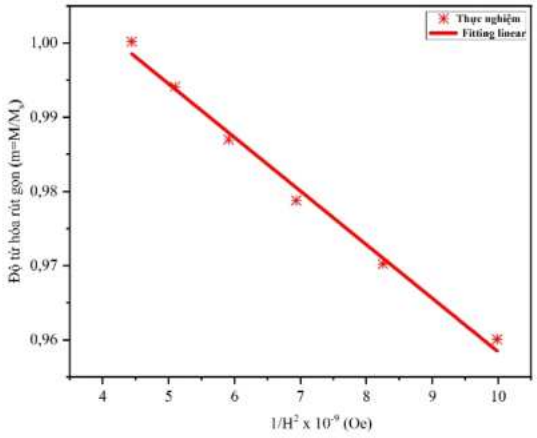

Figure 3.10. Relationship between M/M_s–$1/H^2$ of the Fe_3O_4/PGMA microspheres at large field. The solid line represents linear fitting to the experimental data.

Here, we use the reduced magnetization ($m=M/M_s$), which is a function of $1/H^2$ linearly fitted to equation 2.4 at large magnetic fields (7.96×10^5 - 1.19×10^6 $A.m^{-1}$) (Figure 3.10). Value b – slope of the linear fitting line is used to calculate K_{eff} according to equation 2.7. The estimated value of the effective magnetic anisotropy constant (K_{eff}) of Fe_3O_4/PGMA microspheres at room temperature (300 K) is K_{eff} (LAS) = 2.9 ± 0.6×10^3 (J/m^3). Comparing with K_{eff} (T_B) obtained above, we notice that there is a slight difference (shown in table 2.5); this can be understood based on the temperature dependence of the magnetic anisotropy constant [134,135]. As a result, the magnitude of K_{eff} decreases with increasing temperature so that the K_{eff} (T_B) value at 10 K is larger than the K_{eff} (LAS) obtained at 300 K.

3.1.6.2. Fitting to Langevin function

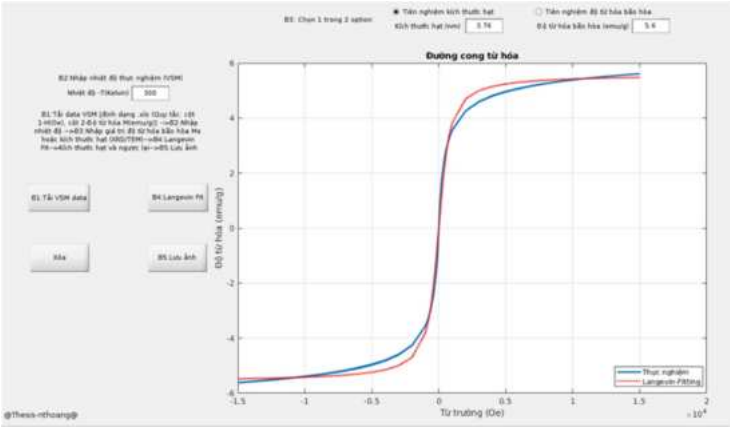

Figure 3.12. The program built in Matlab language to fitting M(H) with the Langevin function.

In order to take advantage of the powerful capabilities of available graphics libraries and create a user interface, the author created a program in Matlab language (Appendix IV) to fit curves from M(H) chemistry of the Fe_3O_4/PGMA microsphere material system is obtained experimentally with the Langevin function to automatically and a priori calculate the size as well as the corresponding standard deviation of the magnetic cores (Fe_3O_4 magnetic nanoparticles) of materials (Figure 3.12).

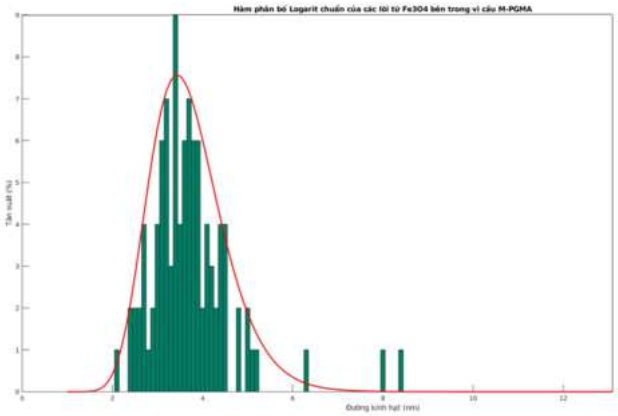

Figure 3.13. Đồ thị kích thước hạt tuân theo hàm phân bố kích thước hạt logarit-chuẩn cho trước.

→ D = 3.76 (nm), σ_D = 0.77 (nm) and the particle distribution function, respectively (figure 3.13). To show the particle size distribution of Fe_3O_4 particles (magnetic core) inside Fe_3O_4/PGMA microspheres, the author writes a program in Matlab language to create specific particle size data following a logarithmic-normal distribution function obtained above (Figure 3.13).

Combined with the FTIR results presented above, the interaction of the PGMA matrix on the Fe_3O_4 magnetic nanoparticles creates a disordered magnetic layer at the surface of the Fe_3O_4 particles (Figure 1). 3.16).

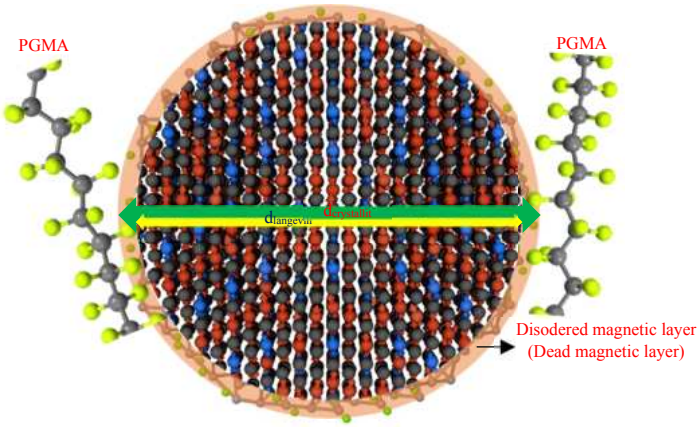

Figure 3.16. Disordered magnetic layer on surface of the Fe_3O_4 nanoparticles.

The primary reason is that the coordination symmetry of metal ions at the surface of Fe_3O_4 nanoparticles is significantly reduced due to the lack of Oxygen atoms, the PGMA molecules filling in the vacancies on the surface of the Fe_3O_4 nanoparticles and occupying the positions of missing atoms, which has led to reducing the spin-orbit coupling. Other authors have reported and discussed similar results, namely Yuan Yuan et al. [136] and Peddis.D et al. [137]. The result is the forming of a dead magnetic/disordered magnetic layer outside the surface of the Fe_3O_4 particles. This disordered magnetic layer is only changed magnetically, but the crystal structure is entirely unaffected. Therefore, we can see that after forming and distributing inside the PGMA matrix, the Fe_3O_4 particles are fixed and subject to the interaction of PGMA molecules, thereby forming a magnetic disturbance layer, leading to the reduced size of the magnetic core. It also contributes to further evidence of the decrease in saturation magnetization of the Fe_3O_4/PGMA microsphere material compared to the bare Fe_3O_4 nanoparticles.

Here, the assumption is that errors (measurement and mathematics) are ignored, and the experimentally measured crystal size is correct (done by the Small-angle X-ray scattering method mentioned before). We can provide a rough model to calculate the thickness of the disordered magnetic layer by $d_{disodered} = d_{crystallite} - d_{Langevin}$ (figure 3.16).

3.1.7. Application of Fe_3O_4/PGMA microsphere material in water treatment

It requires enormous costs and time to carry out complex biomedical applications. At the same time, the author's research facility conditions still need to allow for further research as biomedical applications, so the author preliminarily measured the ability of the Fe_3O_4/PGMA microspheres to adsorb heavy metal ions, specifically Lead ions (Pb^{2+}) - the most abundant and common ion in water sources, especially wastewater from heavy industrial zones. Survey results show that reaching adsorption equilibrium takes about 120 minutes. The Langmuir isotherm equation calculated the maximum adsorption concentration.

The Langmuir model assumes that the adsorption reaction on the adsorbent surface belongs to single-layer adsorption, all adsorption sites are the same, and the adsorbents do not affect each other adsorption site. We perform fitting linear from the experimental points to obtain the explicit form of the Langmuir isotherm equation. Figure 3.17 shows that the Langmuir isotherm adsorption model accurately describes the Pb^{2+} ion adsorption of Fe_3O_4/PGMA (R^2 = 0.99523). From the slope and vertical cutoff point, we calculate the maximum adsorption capacity q_{max} of Fe_3O_4/PGMA for Pb^{2+} ions as 78.2 mg/g and Langmuir constant b = 0.0822 l/mg. From the results, we can see that the Fe_3O_4/PGMA material can remove Lead ions (Pb^{2+}) in water treatment applications.

Here, other isotherm adsorption models, namely Freundlich, Temkin, and Dubinin Radushkevich, have yet to be considered [138,139]. After adsorbing heavy metal ions, these Fe_3O_4/PGMA microspheres were removed using an external magnetic field for deposition and separation. We can desorb and recover Pb^{2+} ions after separation using an HNO_3 acid solution, but the author has yet to do so due to time constraints.

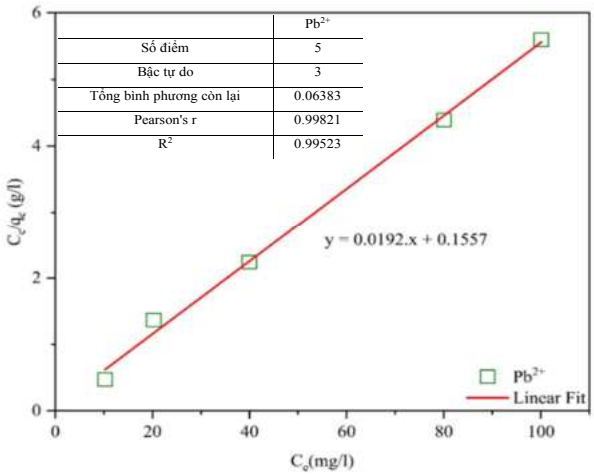

Figure 3.17. Adsorption isotherm line of the Fe_3O_4/PGMA microsphere material for Lead ion (Pb^{2+}).

3.2. Computer simulation results

3.2.1. Monte Carlo simulation

Figure 3.18 shows the pressure constant Monte Carlo simulation results for shaping Fe_3O_4 magnetic nanoparticles inside PGMA microspheres. The simulation reaches equilibrium after 200.000 Monte Carlo steps. The results show that at low pressure (corresponding to when the PGMA microspheres swell), the Fe_3O_4 nanoparticles agglomerate into clusters with large sizes (~850 nm) close to the size of the microspheres. After

the pressure increases (corresponding to the contraction of the PGMA microsphere), the size of the Fe_3O_4 particle clusters decreases almost linearly (in the absence of dipole interactions). Finally, the particle cluster size is formed at approximately 350 (nm).

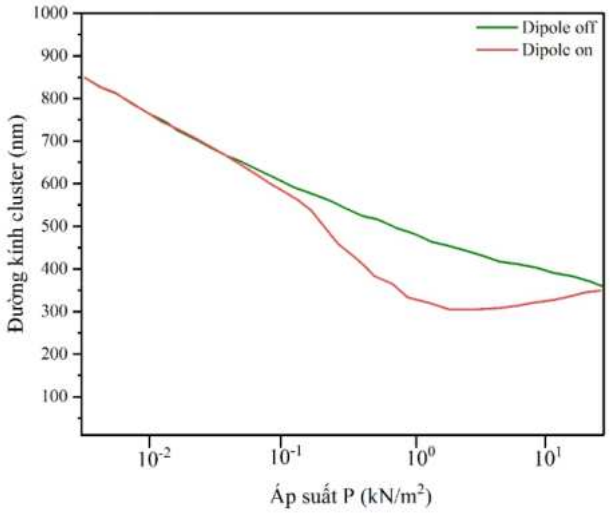

Figure 3.18. Pressure constant Monte Carlo simulation for the forming process the Fe_3O_4 nanoparticles inside PGMA microspheres.

3.2.2. Atomistic spin model simulation

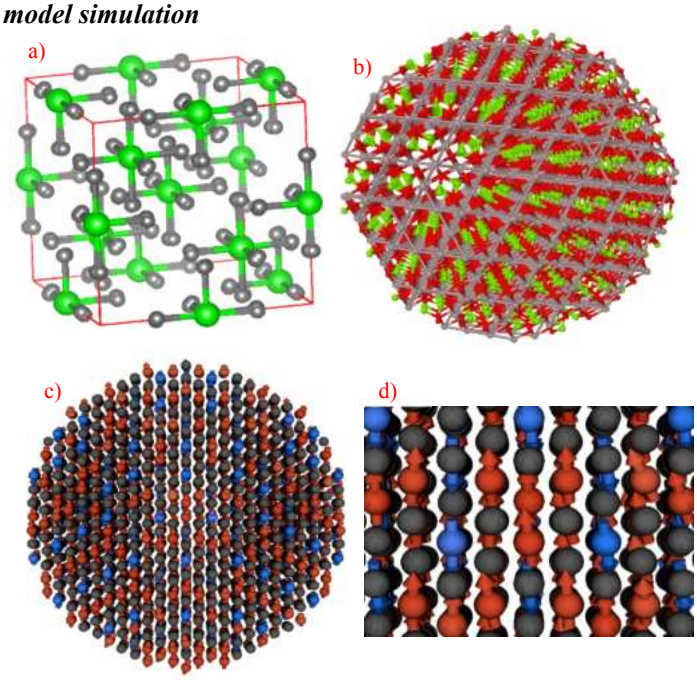

Figure 3.19. a) Unit cell of the Fe_3O_4 material; b) the Fe_3O_4 nanoparticles (d=3.76 nm) c) Spin configuration of one Fe_3O_4 nanoparticle; d) closeup of the spin configuration.

3.2.2.1. Thermal magnetization curve

Checking the accuracy of the simulation and the input parameters are taken from the experiment and numerical calculations presented above and then taken into account in the input file → to simulate the thermal magnetization curve M(T) for reference and comparing the Curie temperature (Tc) with the experimental results (Figure 3.20).

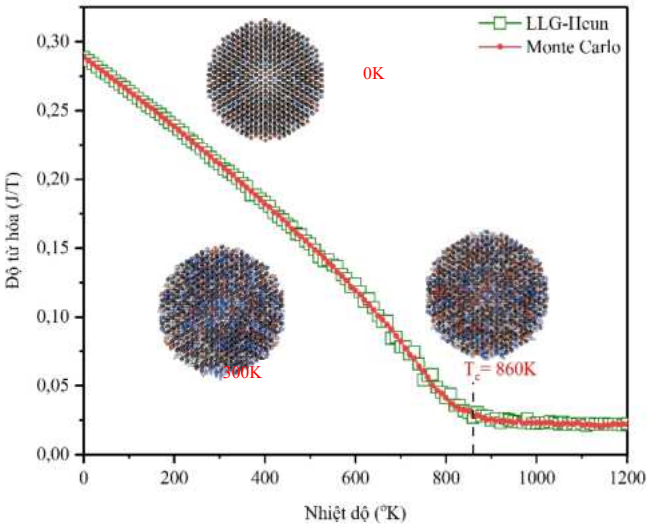

Figure 3.20. Figure 3.20. Simulate the thermal magnetization curve M(T) using two methods: LLG-Heun and Monte Carlo.

Obtained results T_c (simulation) = 860 K~T_c (experiment) = 858 K [141-143] → simulation have a good agreement with the experiment. This proves that the construction of input parameters for the simulation is entirely accurate, thereby proving that the experimental and numerical calculations results obtained above are highly reliable.

3.2.2.2. Effect of dipolar interaction on the magnetic properties of microspheres.

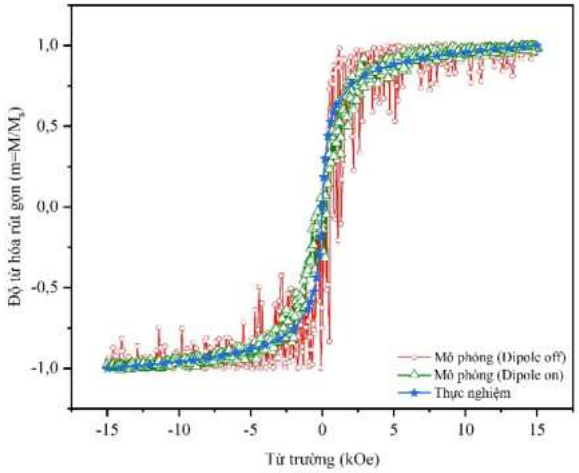

Figure 3.22. Simulation and experimental magnetization curves at room temperature of the Fe_3O_4/PGMA microspheres.

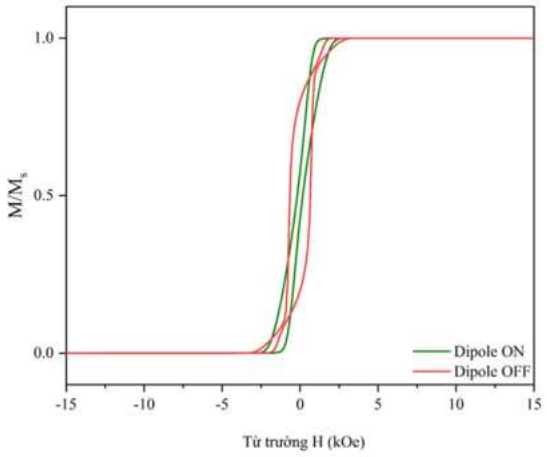

Figure 3.23. Magnetization curves at absolute temperature of the Fe_3O_4/PGMA microspheres.

Figure 3.22 shows that the magnetization curve obtained from the previous experiment matches quite well with the magnetization curve obtained from the simulation → The simulations can represent the actual material system (the Fe_3O_4 nanoparticles inside Fe_3O_4/PGMA microspheres). In addition, we find that the

experimental magnetization curve fits better with the simulated magnetization curve (Dipole ON) → In fact, Fe_3O_4 particles still have dipolar interactions despite being fixed in the PGMA matrix.

Eliminate thermal effects on the Fe_3O_4 magnetic nanoparticle system → simulate the magnetization curve of the sample at absolute temperature (0 K) (Figure 3.23). The results are opposite to those at room temperature (300 K); the particles reach saturation at lower fields in the presence of dipolar interaction (blue line - figure 3.23). The coercivity is smaller and tends to decrease as it approaches the weak field, which is the opposite of the case where there is no dipolar interaction (red line - figure 3.23).

3.2.2.3. Interparticle spacing dependence magnetic properties of microspheres.

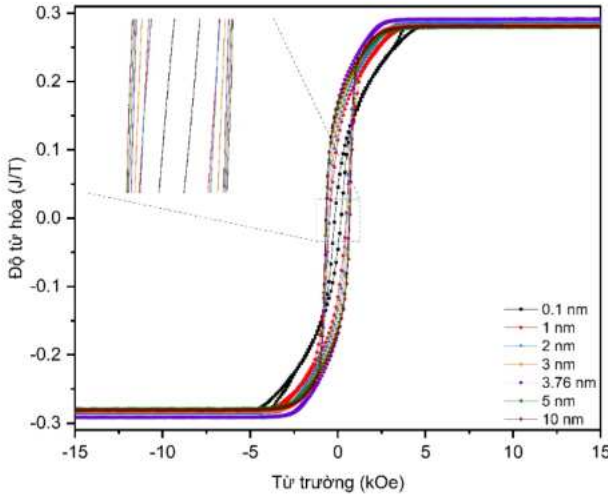

Figure 3.27. Magnetization curve of the Fe_3O_4/PGMA microspheres at 0 K, exists of dipolar interaction with different interparticle spacing.

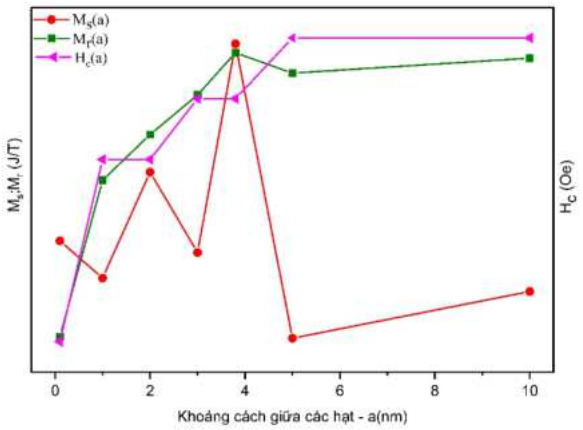

Figure 3.28. Interparticle spacing dependence magnetic properties of microspheres.

→ Optimal spacing between Fe_3O_4 magnetic nanoparticles to ensure performance for each application. Specifically, this optimal condition is meaningful for biomedical applications requiring large saturation magnetization (M_s) but small H_c, such as targeted drug delivery, where the optimal distance is 3.6 nm (equal to its physical size). However, for biomedical applications requiring large H_c coercivity (hyperthermia) or torque amplitude (microfluidics, lab-on-chip), the optimal distance is 5 nm.

3.2.2.4. Particle size dependence magnetic properties of the microspheres.

Perform simulation of magnetization curve of Fe_3O_4 particles at 0 K with particle size changing from 3.76 nm (current size) to 20 nm (below critical size) (Figure 3.29) → particle size increases from 3.76 - 15 nm, the saturation magnetization first decreases, at the same time the remanence M_r and coercivity H_c increase (figure 3.30) → We can predict the experiment for Fe_3O_4/PGMA microspheres to ensure that the size of the Fe_3O_4 magnetic nanoparticles must be 3-8 nm for the superparamagnetic state requirement. Furthermore, we can also a priori consider the optimal conditions for some biomedical applications requiring large saturation magnetization (M_s) but small H_c, such as targeted drug delivery; the optimal Fe_3O_4 size is 3.76 nm (equal to the actual size of the Fe_3O_4 particles being considered). However, for biomedical applications that require a high amplitude of H_c coercivity (hyperthermia) or a high amplitude of torque (microfluidic systems, lab-on-chip), the appropriate Fe_3O_4 size is 10-20 (nm).

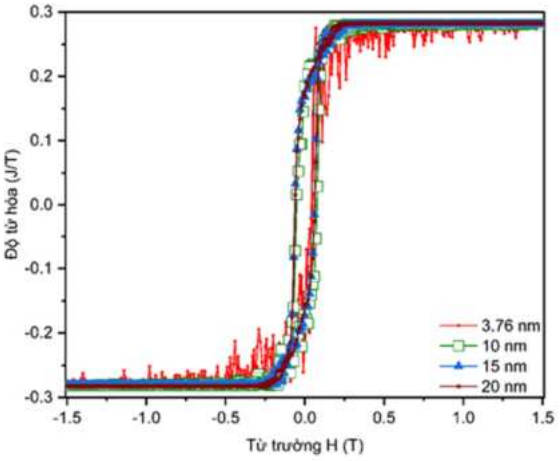

Figure 3.29. Magnetization curves of the Fe_3O_4/PGMA microspheres for various particle size of the Fe_3O_4 nanoparticles (at 300 K).

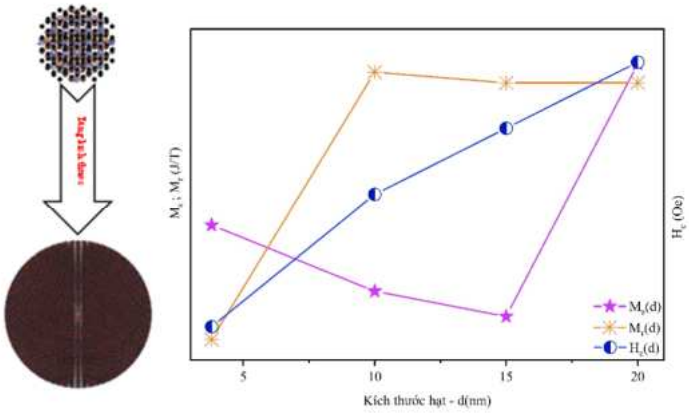

Figure 3.30. Dependence of magnetic properties of the Fe_3O_4/PGMA microspheres to particle size of the Fe_3O_4 nanoparticles.

3.2.2.5. Role and influence of dipolar interaction on blocking temperature.

Figure 3.31 shows the simulation results of the Zero-Field-Cooled (ZFC) magnetization curve (without external magnetic field) of Fe_3O_4/PGMA microspheres with (Dipole ON) and without (Dipole OFF) of dipolar interactions. They show that the magnetic dynamic behaviour of the material in both cases is quite similar (the difference is not much), spanning from the average low-temperature region to the high-temperature region. However, at an absolute temperature of 0 K, the magnetization in the presence of a dipolar field is much lower than in the absence of a dipolar field.

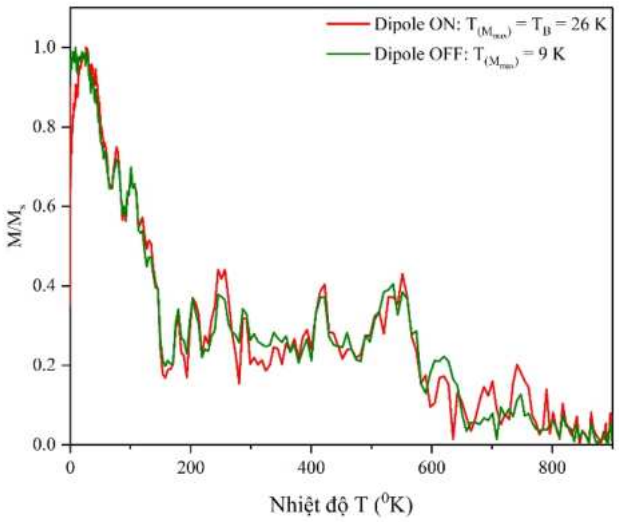

Figure 3.31. ZFC magnetization curve of Fe3O4/PGMA microspheres with/without of dipolar interaction.

The temperature corresponding to the maximum magnetization recorded is 26 K and 9 K, respectively, corresponding to the Dipole ON/Dipole OFF state. In the presence of a dipole field, at absolute temperature, observing the spin configuration of the particle (Figure 3.32a) shows that the spin of each particle is entirely parallel and oriented along the easy anisotropy axis of each particle (because, at this time without thermal

effects from the external environment and external magnetic field energy, the anisotropic field will then become dominant). However, the total magnetization moment of all particles in the system is close to 0 (due to the ease of each particle having a different direction leading to $\vec{M} \sim 0$, the nanoparticles are now "frozen" and locked in this state, this phenomenon is called spin-glass-like [151,152]. When heated, the degree continues to increase after reaching the maximum magnetization at a temperature of 26 K (Figure 3.32b - the spin of the entire particle is almost parallel and aligned), and a slope appears (decrease in magnetization). The reason is that the dipole interaction between Fe_3O_4 magnetic nanoparticles creates a dipole field (H_{dip} - a demagnetization field) and contributes to the crystal field, leading to a decrease in the system's free energy. The result is the emergence of a stable state with a high energy potential barrier, which causes the magnetic nanoparticles' unblocking kinetic behaviour. An experimental study has also been reported with similar results [153]. On the contrary, no slope appears at the blocking temperature region when the dipole field is turned off (Dipole OFF), indicating no unblocking kinetic behaviour of Fe_3O_4 magnetic nanoparticles. As a result, the T_B value shifts when changing the particle concentration.

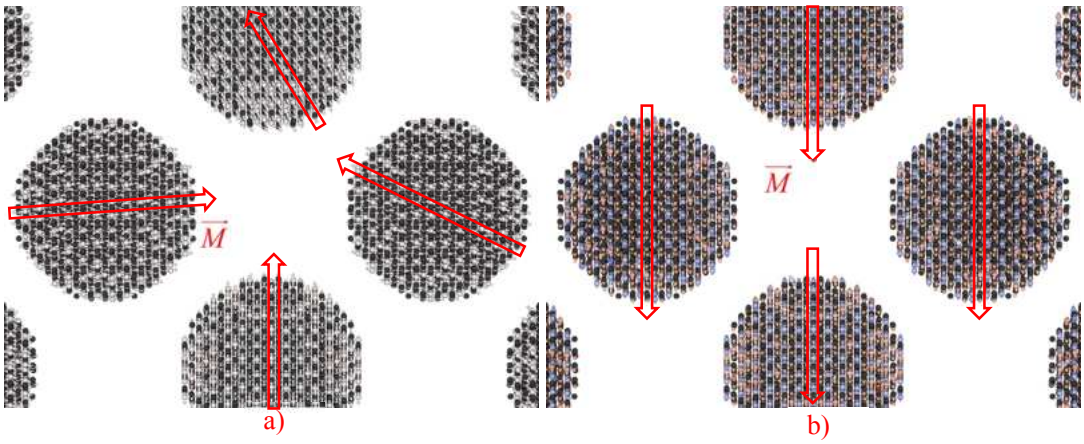

Figure 3.32. Snapshot of magnetic spin configuration in ZFC curve simulation with existence of dipolar interaction: (a) at 0 K; (b) at T_B.

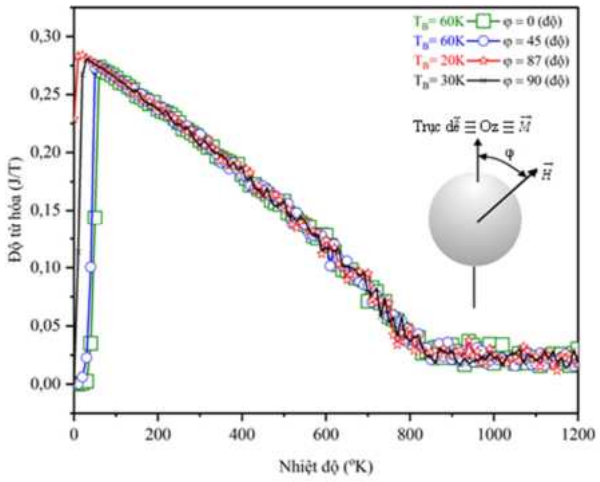

Figure 3.33. ZFC magnetization curve of the Fe_3O_4/PGMA microspheres at different azimuth angles φ.

Our study delves into the simulation of the ZFC magnetization curve at various azimuthal angles φ, a topic that has not been extensively explored in the context of ferromagnetic materials. Notably, our findings at angle $\varphi = 87^o$, corresponding to T_B= 20 K, align entirely with the average value from previous experiments.

Furthermore, we observe slight variations in the T_B value at different azimuth angles, such as $\varphi = 0^o$ and $\varphi = 45^o$, where $T_B = 60$ K (figure 3.33).

Our conclusion, while significant, also raises important questions that warrant further investigation. The observed differences in the obtained T_B value depending on the initial external magnetic field direction or the sample placement/easy axis distribution of the magnetic nanoparticle before measurement, as reported by author Joshi and colleagues [157] for antiferromagnetic materials $Fe_{0.6}Zn_{0.4}F_2$, have not been thoroughly explored for ferromagnetic materials such as Fe_3O_4. To validate our predictions, conducting specific experimental studies on ferromagnetic materials is crucial, enhancing our findings' reliability.

Our findings have significant implications for practical applications, particularly in hyperthermia. For instance, the effectiveness of hyperthermia therapy is directly linked to the specific absorption rate (SAR) [158-160], which is the anisotropic energy density/anisotropy constant. Given that the blocking temperature (T_B) is proportional to the effective magnetic anisotropy constant (K_{eff}), we can infer that a high T_B is essential for efficient local hyperthermia. Suppose we use the Fe_3O_4/PGMA microsphere material for local hyperthermia applications with a heat source using an alternating external magnetic field and ensure that the angle φ always equals 0 or 45°. In that case, we can significantly increase the treatment efficiency, which will reach the optimal maximum (with $T_B = 60$ K).

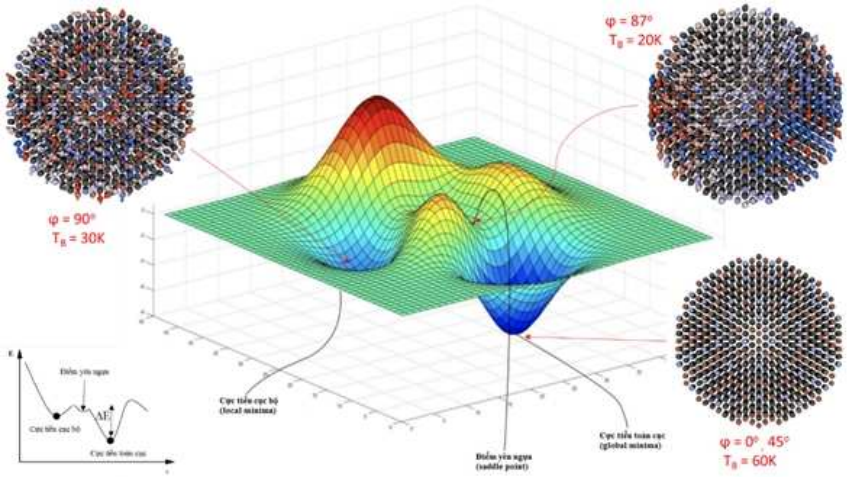

Figure 3.34. Energy diagram (2D and 3D) of the Fe_3O_4 nanoparticles during the process Zero-Field-Cool magnetization curve measurement.

3.2.2.6. Torque of the Fe_3O_4/PGMA microspheres material

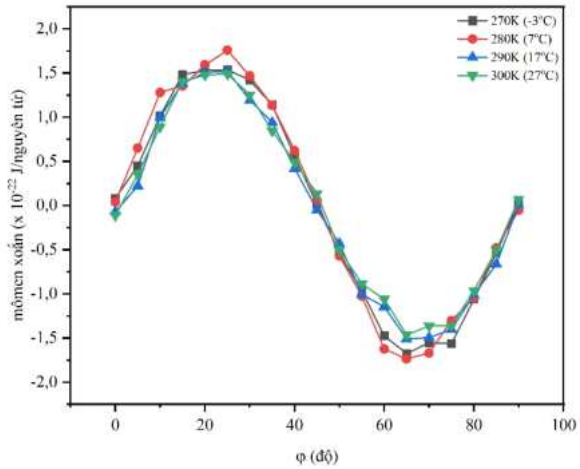

Figure 3.36. Torque of the Fe_3O_4/PGMA microspheres at sub-region around room temperature (300 K)

Investigation of the torque of the material system aimed at lab-on-chip applications → investigation of the torque of Fe_3O_4/PGMA microspheres at different temperatures near room temperature and different angles different φ positions (from 0-90°) (Figure 3.36, Figure 3.37).

Figure 3.36 shows that the torque reaches its maximum at the angle φ = 70° at a temperature of 310 K (37 °C). Interestingly, this value is the same as the standard human body temperature. As a result, we have a priori suggestion that for in vivo applications, the Fe_3O_4/PGMA microspheres material will achieve maximum amplitude of torque at the standard human body temperature value. This has implications for biomedical applications that use external magnetic fields; as mentioned above, although we cannot change the direction of the particle's anisotropic axis, it is possible to change the direction of the applied magnetic field so that the torque reaches an optimal maximum.

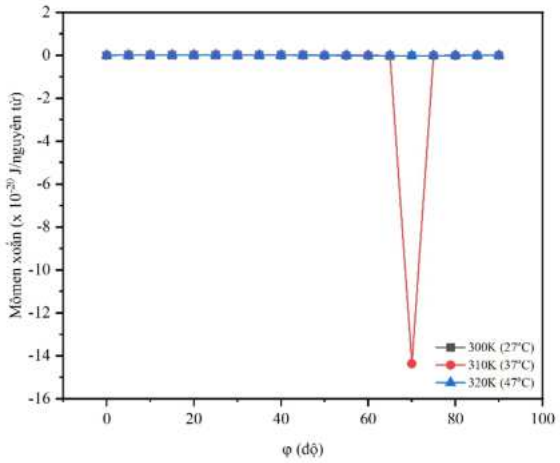

Figure 3.37. Torque of the Fe_3O_4/PGMA microspheres in the vicinity above room temperature.

→ The significance for clinical experiments and inclusion in biomedical applications is as follows: for microfluidics and lab-on-chip applications, the suitable temperature range is from (-3 C) to 27 °C, ensuring the azimuth angle φ = 65° and 25° for optimal maximum torque. Besides, we can build a standard database for calibration to qualify/quantify various biological elements. However, this needs to be coordinated with experimental biomedical experiments. Additionally, for in-vivo applications, namely targeted drug delivery or local hyperthermia, combined with the blocking temperature (T_B) survey simulation results discussed above, we have it can be stated a priori that the initial temperature should be 37 °C, the azimuth angle φ should be guaranteed to be 60-70° for the material to reach maximum torque, thereby achieving the best possible application performance. In addition, we can also a priori predict that the storage conditions for Fe_3O_4/PGMA microspheres for these biomedical applications should be in the range of (-3 °C) to 27 °C for the material to be best preserved before use. Put into use, this is entirely consistent with the overview report of author Chong Li and colleagues [161].

CONCLUSIONS AND RECOMMENDATIONS

Conclusions:

The magnetic properties of composite materials used in biomedicine are crucial for applications involving external magnetic fields and assessing application effectiveness. Investigating and quantifying these properties, namely magnetic anisotropy constant, torque, blocking temperature, and dipolar interactions, is necessary to implement applications, particularly in biomedicine. This thesis introduces a groundbreaking

model that combines experiment, theory, and computer simulation to study the magnetic properties of the Fe_3O_4/Poly(glycidyl methacrylate) microsphere material, offering a fresh perspective in the field.

Using experimental methods, the author has synthesized a monodisperse spherical Fe_3O_4/Poly(glycidyl methacrylate) microsphere material with a narrow size distribution of 1.36 ± 0.09 μm. The Fe_3O_4 nanoparticles are shaped and distributed fixedly inside/on the surface of the PGMA polymer matrix (with D = 3.76 nm, σ_D = 0.77 nm) following a logarithmic-normal distribution function. Under the influence of dipolar interactions, it agglomerates into clusters of ~ 350-800 nm in size. The PGMA polymer interacts with the surface atoms of the Fe_3O_4 magnetic nanoparticles to form a disordered magnetic layer, leading to a decline in the magnetic properties of the Fe_3O_4/Poly(glycidyl methacrylate) microsphere material compared to the bare Fe_3O_4 material. Microspheres are superparamagnetic, saturation magnetization M_s = 5.61 emu/g, remnant magnetization M_r = 0.015 emu/g, and coercive field H_c = 1.42 Oe. Based on experimental data, the theoretical calculation of the effective anisotropy constant (K_{eff}) is determined to be K_{eff} (T_B) = 1.9 ± 0.15×10^4 J/m^3 and K_{eff}(LAS-300 K) = 2.9 ± 0.6 ×10^3 J/m^3. This shows that K_{eff} depends on particle size and temperature. The synthesized Fe_3O_4/PGMA microspheres can adsorb Lead ions (Pb^{2+}) with a maximum adsorption rate of 78.2 mg/g according to the Langmuir isotherm model.

Based on experimental data, the simulation results have not only provided insights into the intrinsic micromagnetic parameters of the Fe_3O_4/PGMA microsphere material under regular and special conditions but also practical implications. These findings suggest optimal conditions for biomedical applications such as targeted drug delivery and local hyperthermia, thereby demonstrating the potential of the research to benefit these fields directly. The microspheres can be effectively utilized in these applications by controlling the direction of the external magnetic field and the temperature.

This research model, while promising to other composite materials, which have structures similar to Fe_3O_4/PGMA microspheres, requires further empirical studies to fully confirm its accuracy. The results have been cross-referenced with other scholars and validated, but additional research is necessary to strengthen these findings. These results, however, serve as a solid foundation for future research on materials with similar structures, opening up new avenues for exploration in the field.

Recommendations:

To develop the research direction of the thesis, we can make changes to the input files and repeat the simulations performed in the thesis (simply by programming shell/bash script), specifically by changing the shape/type of nanoparticles from within the PGMA base material. In addition, this research model can also be applied to many other composite materials with similar structures to build a data set from which machine-learning techniques can be used to train the computer to automatically calculate, perform simulations and classify data, providing valuable prediction for the experimental/clinical experiment process. Hybrid computing platforms similar to grid computing are suitable and recommended to develop this research direction.

NEW CONTRIBUTIONS OF THE THESIS

-The thesis has built a multidimensional model to study magnetic properties applied to magnetic microsphere material Fe_3O_4/Poly(Glycidyl Methacrylate) by combining experiment, theory and computer simulation. From there, we provide a priori for experimental and specific clinical experiments for the Fe_3O_4/PGMA microsphere material.

-This research model can be applied to other composite materials with structures similar to Fe_3O_4/PGMA microspheres.

LIST OF THE PUBLICATIONS RELATED TO THE DISSERTATION

1. Nguyen Le Hoai Phuong and Nguyen Thanh Hoang, *Synthesis and characterization of Fe_3O_4@Poly(*glycidyl methacrylate*) nanocomposite for removal of toxic heavy metal ions from aqueous solution*, Trade and science-technology development in the MeKong delta in the context of international integration proceeding, 2019, ISBN 978-604-965-263-9, pp. 304-309.

2. Hoang Thanh Nguyen and Tuan Manh Nguyen, *Investigation of Magnetic Properties of Magnetic Poly (*glycidyl methacrylate*) Microspheres: Experimental and Theoretical*, Advances in Materials Science and Engineering, ISSN 1687-8442, 2021, 2021, 6676453.

3. N.T. Hoang, N.L.H. Phuong and N.M. Tuan, *Particle size dependence magnetic properties of nanofluids based on magnetite nanoparticle: A computer simulation study*, HCMUE Journal of Science, 20(3), pp. 458-467, 2023

4. N.T. Hoang, T.N. Lan, N.M. Tuan, *Effect of dipolar interaction on magnetic properties of magnetite nanoparticles system: a simulation study,* Communications in Physics, 33(3), pp. 285-296, 2023.

5. Nhan Tri Tran, Hoang Thanh Nguyen & Lan Nguyen Tran, *Reaching high accuracy for energetic properties at second-order perturbation cost by merging self-consistency and spin-opposite scaling*, The Journal of Physical Chemistry A, 128 (8) pp. 1543-1549, 2024.